

UNIVERSITÄT FREIBURG
ADVANCED PHYSICS LAB COURSE
FP1 2024-2

Experiment 10 Laser Gyroscope

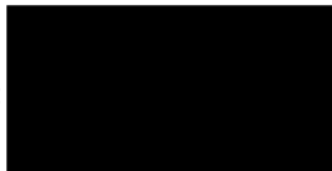
Short Report



September 8, 2024

Lab Work conducted: August 4 & 5

Assistant:



Contents

1 Objectives	2
2 Equipment used	2
3 Part 1: Setting up the Laser Gyroscope	3
3.1 Procedure and Observations Part 1	3
3.2 Discussion Part 1	4
4 Part 2: MEMS Gyroscope in a Smartphone	5
4.1 Procedure Part 2	5
4.2 Data Analysis Part 2	6
4.3 Discussion Part 2	8
5 Conclusion	9
6 Appendix A: Signed Lab Notes	10
7 Appendix B: Additional Pictures and Data	14

1 Objectives

A laser gyroscope is used in many applications for sensitive rotation measurements (see examples in [Dem17] [Geb+20]). The aim of this experiment is to give an insight into the functioning of such gyroscopes. In addition to attempting to set up a laser gyroscope, we use its rotating platform to test the electro-mechanical gyroscope sensor of a smartphone and compare the angular velocities obtained with the nominal values.

2 Equipment used

We use the pre-assembled laser gyroscope kit by *eLas* [Las] shown in fig. 1. A rotating platform forms the foundation of a ring laser system consisting of a He-Ne laser tube, three mirrors and a quartz glass etalon. The light is then coupled out through one of the mirrors and is directed so that the two laser beams - clockwise and counterclockwise waves - realign and interfere in a beam splitter (BS). The two outputs of the beam splitter are analysed using two photodiodes, an amplifier, an oscilloscope and a frequency counter. The angular frequency and direction of the platform rotation can be preset on a velocity control device.

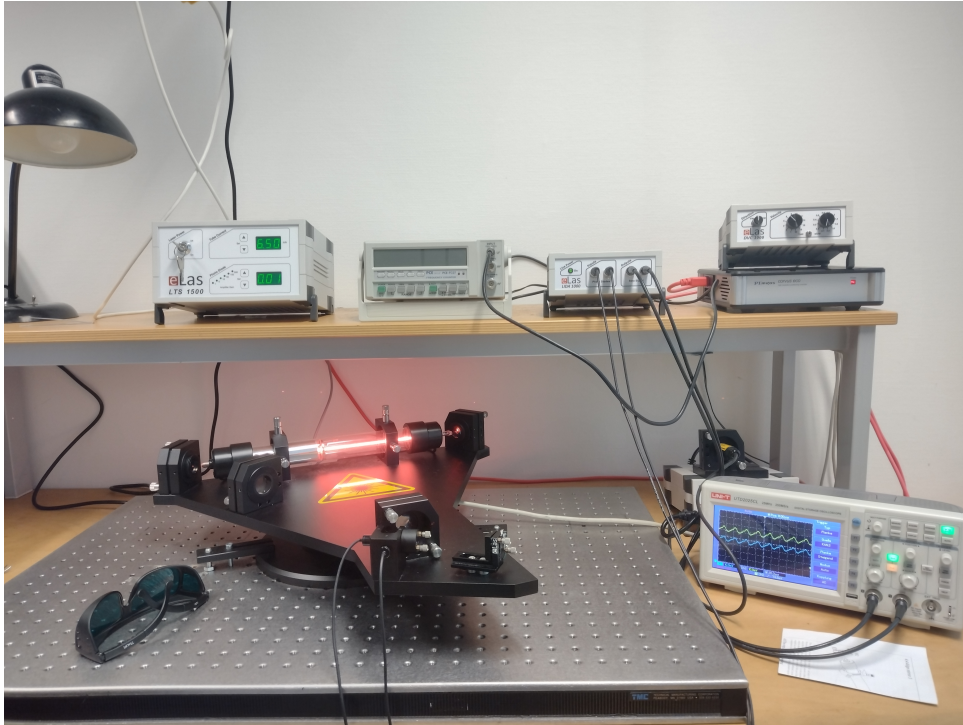


Figure 1: Setup of the laser gyroscope

According to the definition provided in chapter 1 of [Luh], the laser gyroscope used in this experiment can be classified as being *active*, as the active medium and cavity of the laser are part of the rotating system and the output is a change in beat frequency $\Delta\nu$, which is proportional to the angular velocity ω , at which the system is rotating. In *passive* laser gyroscopes, on the other hand, the laser light is created outside of the rotating system and guided there using fibre optics, in which case the output is a phase shift $\Delta\phi$, which is again proportional to the angular velocity ω .

Which type of laser gyroscope is most suitable, depends on the application. Active laser gyroscopes are known to achieve very high precision [Luh], but are quite difficult to set up, as we will see in part 1 of this report, and require expensive optical components, like high-quality mirrors. We speculate that the extremely high precision is due to several factors, like the high coherence of the laser light in the rotating cavity, or the fact that frequency differences are simply easier to measure precisely than phase shifts. In the here conducted experiment, this very precise measurement of frequency change would have been achieved by measuring the beat frequency at two points with a 180° phaseshift between them and then use a comparator unit in order to create a logical TTL signal. Another downside of active laser gyroscopes is that they are comparatively heavy and

probably difficult to build on a very small scale. Additionally, there is a phenomenon called the "Lock-in-Effect" [Las], which limits the operation of the active laser gyroscope to angular velocities higher than a certain threshold $\omega_{\text{Lock-in}}$, below which the two gyrating modes couple due to unavoidable scattering at the resonator mirrors.

Passive laser gyroscopes tend to be a bit lower in their precision, but are easily assembled using cheaper components and do not have the problem with the "Lock-in-Effect".

3 Part 1: Setting up the Laser Gyroscope

During the two designated lab days, we did not actually get to a point where the whole laser gyroscope was working correctly and were thus unable to take any real measurements with it. However, the process of trying to set up and optimise the components of the gyroscope was highly educational. In the following, we will be presenting and describing the steps undertaken, as well as discuss the main limitations we were facing.

3.1 Procedure and Observations Part 1

For the sake of simplicity, we will be referring to the different optical components by the names used in the manual [Las] (compare fig. [12] in Appendix B).

On the first day of lab work, the ring laser was already correctly assembled and lasing with a satisfactory laser power, so what remained to do for us was to select a mode via the etalon and to align the light paths after the out-coupling, around the beam splitter, to get interference signals in the photodiodes.

By rotating the etalon slightly around the optical axis, one of the modes was quickly found and lasing set in. Following the advice given in chapter 6.1 of the lab instructions [Las], it was first confirmed that this was indeed the central mode (as no other reflections on M1 or M2 were visible) and the etalon was tilted carefully by an angle until lasing had briefly stopped and set in again, this time in a higher (and more stable) mode.

Next, one of the photodiodes was removed and the two red dots leaving the opening were observed on a screen, as shown in fig. [2]. By moving the screen back and forth on the line of the beams and observing their divergence in horizontal and vertical direction, the beams were rendered horizontally parallel by turning the screws on the beam bending mirror (BM) and vertically parallel by tilting the BS cube. After this was achieved, we tried to get the dots to overlap and interfere by translating the BM. These steps were repeated iteratively a few times.

Even though an interference pattern was initially visible on the screen and we managed to reduce the number of interference lines to obtain an almost perfectly homogeneous single interference spot on the screen, the oscilloscope output showing the pre-amplified signals from the two photodiodes did not look at all as expected. On both channels, a periodic signal was visible, as can be seen in fig. [3]. This signal did, however, not change at all when rotating the table and besides the two curves stayed in phase with each other all the time. The observed signals can therefore not stem from interference, but seem to stem from other sources unrelated to the actual experiment, like influences of electronics and similar.

Already during the steps described above it was noted, that there seemed to be some sort of drift in the system, as the lasing stopped a few times, but could at first always be re-established quite easily by slightly changing the angle of the etalon. At some point, however, the lasing stopped entirely and could only be regained by removing the etalon completely. This made us first draw the conclusion, that the etalon itself would be the problem.

After the etalon and other optical components had been cleaned and it was confirmed that there was no obvious damage to the etalon, different systematic approaches were attempted with the goal of finding the correct positioning and tilt of the etalon. One of these systematic approached was, for instance, to first turn the θ -screw of the etalon holder by a tiny bit, then move the ϕ -screw slowly through its full range, while simultaneously rotating the etalon around its axis and repeating the whole procedure for the next θ position. These attempts were, however, unsuccessful. One possible explanation for this was, that the laser was at this point only operating slightly above laser threshold and that the etalon did introduce too strong of a loss to keep up the lasing.

Consequently, the decision was taken to redo the general alignment of the laser, for which the green laser module was mounted behind M3 and the etalon was removed. The alignment was checked

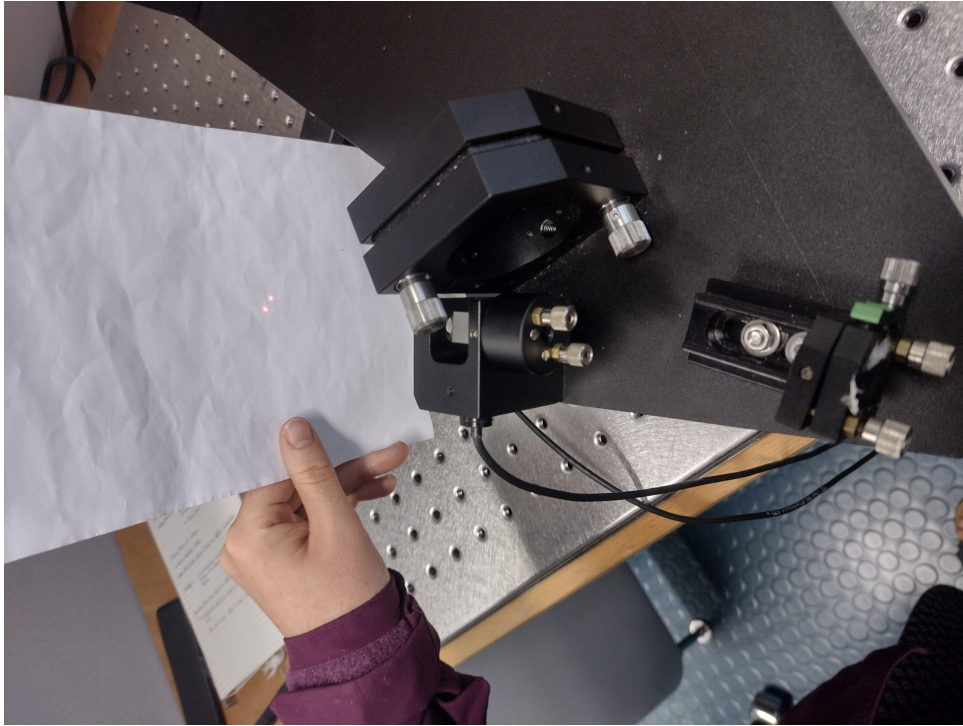


Figure 2: Beams at one of the photodiodes before alignment

and adjusted in the order suggested in chapter 6 of [Las](#), thus starting with making sure that the green alignment laser passes the capillary within the laser tube without touching the walls, that it hit the three mirrors in their centres and that the front side reflections were used at all aligned reflections. After the lasing threshold was reached, the laser power was optimised by going through all the screws one at a time and slightly correcting them, so that an increase in signal strength could be observed on the oscilloscope. The laser was then also visually operating at much higher power than before.

Next, the etalon was brought back into the beam path. By carefully rotating and tilting the etalon in the hand, without fixing it in the holder, it was possible to find a position in which the laser starts lasing. The problem was, though, that once one pushed the etalon into its holder, lasing stopped again. A solution was found by loosening the etalon holder and moving the complete holder with the etalon in it, until a correct position was found and stable lasing commenced.

Finally, we attempted to once more achieve perfect interference in the two beams reaching the photodiodes, but did unfortunately not manage this within the designated lab hours.

3.2 Discussion Part 1

Even though the laser gyroscope was never fully running and no measurements could be taken with it, we did gain a good insight into how such a device needs to be set up and aligned correctly and learned about a few important points to be aware of for successful laser operation.

To begin with, we learned how to align the different optical components using an alignment laser in a different wavelength and how to observe laser beams leaving the ring laser on screens at different distances from the setup.

One of the main take-away learning experiences was the insight of how important it is to maximise the laser output, even after the lasing limit had been reached. We learned how to do this in a systematic and effective manner by only changing one variable (i.e. the angle of one optical component) at a time and by observing the change in output signal strength with a suitable oscilloscope operation mode.

Furthermore, we were made aware how incredibly sensitive the whole setup is and how factors like placing a hand on any of the components can immediately kill lasing. It was also striking how sensitively the position of the etalon had to be chosen for the laser to work. Similarly, it was interesting to observe how strongly the system was subject to environmental influences, like changes in the temperature.

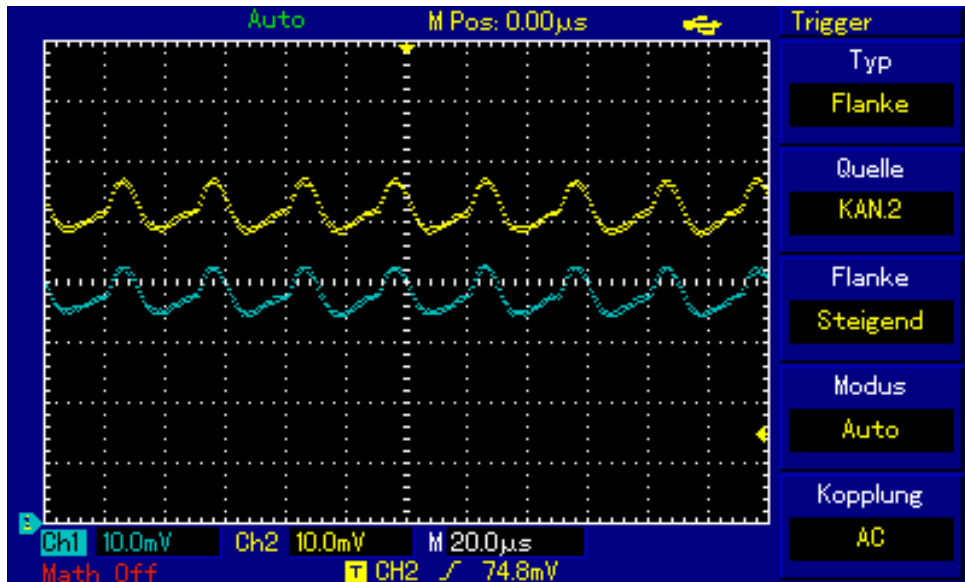


Figure 3: Pre-amplified signals of the two photodiodes.

We are not entirely sure, why it was not possible to observe the expected sinus signals with a 180° phase shift on the oscilloscope when rotating the gyroscope. One possible explanation is that the interference created between the two beams reaching the photodiodes was not yet optimal. If one had more time at hand, one would need to very carefully optimise the alignment of those beams by manipulating the BM and the BS in order to make them fully parallel and overlapping.

4 Part 2: MEMS Gyroscope in a Smartphone

In this part of the experiment, the application *Phyphox* was used to take data with the built-in gyroscope of a smartphone and compare this with the nominal velocities of the rotating platform as given in the manual [Las](#).

The smartphone used for this experiment has a micro-electro-mechanical sensor (MEMS) gyroscope. More specifically, according to the information accessed via *Phyphox*, it is part of a motion sensor package of the series ICM-4x6xx produced by *TDK-Invensense*. The exact version is not known to us, but an exemplary datasheet for one of those devices is given in [Inv](#). The only information they give about the physical functioning of the gyroscope is this:

”When the gyroscope is rotated about any of the sense axes, the Coriolis Effect causes a vibration that is detected by a capacitive pickoff” ([Inv](#), p.36),

so we refer to [Gil+22](#) for further explanations about that. In general, MEMS gyroscopes use a constantly vibrating proof mass that is deflected by the Coriolis force when a rotation occurs. Sensing electrodes detect this change in movement. The deflection’s magnitude can then be used to quantify the Coriolis force $F \propto \omega$ and therefore also the angular frequency ω of the rotation.

4.1 Procedure Part 2

A smartphone with the *Phyphox* application was placed in the centre of the rotateable laser gyroscope platform as shown in [fig. 4](#)

Then, the platform was rotated for a short amount of time in alternately the clockwise (cw) and counter clockwise (ccw) direction. This was conducted for 12 different angular velocity settings. For angular velocities labelled as ”fast”, the rotation time was chosen to be around 5 s and for the ”slow” velocities this was increased to approximately 10 s to account for the increased noise. In addition, we took a measurement without rotation for approximately 20 s. The data obtained was extracted from *Phyphox* and loaded into python for further analysis.

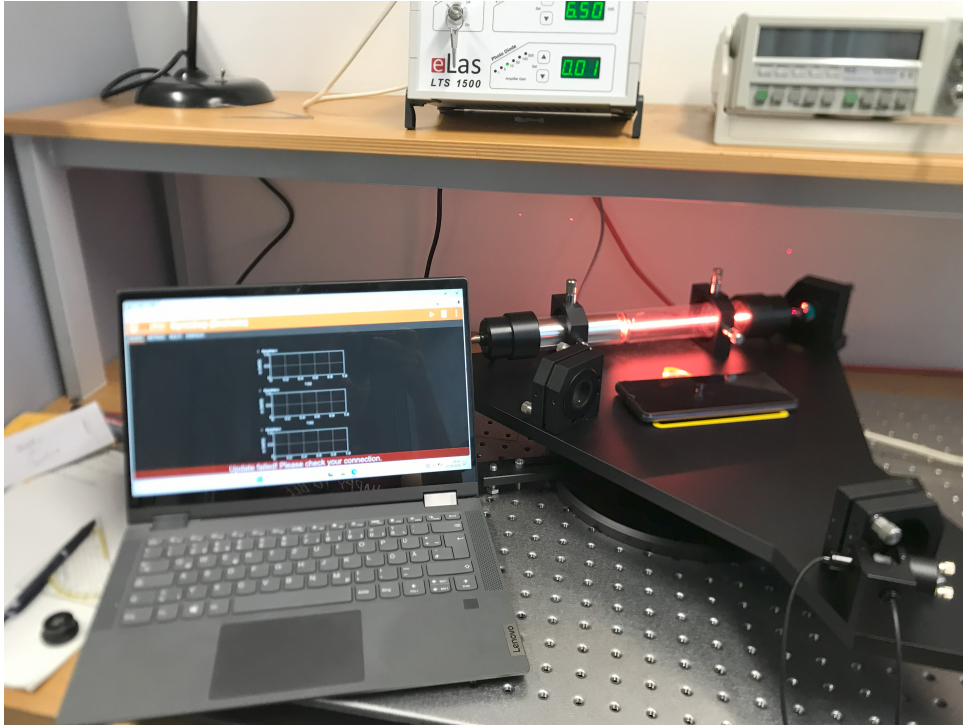


Figure 4: Setup for the measurement with the smartphone gyroscope. *Phyphox* was operated remotely from a laptop.

4.2 Data Analysis Part 2

The angular velocity settings chosen at the stepper motor can be found in *Table 1* of the lab notes (fig. 9). The reference values for the angular velocities ω_c are not given exactly by the labels on the velocity controller, but the precise values and their uncertainties are listed in chapter 5 of [Las](#).

The complete data from the smartphone sensor - the vector components ω_x, ω_y and ω_z as well as the absolute value ω_{tot} of the measured angular velocities - are visualised in figs. 13 and 14 in Appendix B. The time resolution is around 2 ms, the resolution in $\omega_{x/y/z}$ is approximately $0.06^\circ/\text{s}$. The coordinate system used for the x, y, z -labels is defined such that the z axis is the vertical one and is thus primarily interesting for us. Negative values correspond to a clockwise rotation, positive values mean a counterclockwise rotation.

Since we started data acquisition before the start of the rotation, we have to select the relevant time periods manually. We do this visually, by looking at the plots and identifying roughly when the table started rotating and when it stopped, respectively (see "analysed interval"s in figs. 13 and 14). Within the selected regions of interest, we then calculate the mean of the measured angular velocities. The uncertainty of a mean value $\hat{\omega}$ is calculated via

$$\sigma_{\hat{\omega}} = \sqrt{\frac{1}{N(N-1)} \sum_{i=1}^N (\omega_i - \hat{\omega})^2}.$$

However, this uncertainty might not be sufficient to describe statistical fluctuations: To check for a potential shift in time, we have taken the $(20^\circ/\text{s})$ -ccw-measurement twice - at the very beginning and at the end of the measurement series. The mean values $\hat{\omega}_z$ from these measurements deviate from each other by $\approx 0.02^\circ/\text{s}$, which is significantly larger than their calculated uncertainties $\approx 0.004^\circ/\text{s}$. If we include this additional uncertainty into our analysis, it dominates all of the uncertainties calculated above (which are all smaller than $0.006^\circ/\text{s}$), so that we effectively use a statistical uncertainty of $\sigma_{\hat{\omega}} = 0.02^\circ/\text{s}$ on all mean values in the following.

We also check for a potential systematical error that would come from a constant offset in the

measured data. For this, we analyse the zero-velocity-measurement, where we get the mean values

$$\begin{aligned}\hat{\omega}_x &= 0.008(20)^\circ/\text{s}, \\ \hat{\omega}_y &= 0.003(20)^\circ/\text{s}, \\ \hat{\omega}_z &= -0.005(20)^\circ/\text{s}, \\ \hat{\omega}_{\text{tot}} &= 0.090(20)^\circ/\text{s}.\end{aligned}$$

The offsets in x , y and z are not significant and are probably mere statistical fluctuations, whereas the absolute value has a more significant offset. This offset is not unexpected since the absolute value has per definition an asymmetrical distribution (no negative values to compensate for positive statistical fluctuations) and hence a bias towards values > 0 .

This bias also means that ω_{tot} is not a good measure for our purposes (comparing ω with ω_c), at least for small velocities. Ideally, we would calculate the projection on the rotation axis and compare its mean with ω_c . In our case, the rotation axis corresponds approximately to the z axis, so that we can use just the z component instead. We check that this approximation is indeed close enough by comparing the vector components in fig. 5. Clearly, the rotation axis is not perfectly parallel to the z -axis since all three components vary linearly with the set angular frequency. The z component, though, is more than a hundred times larger than the other two. Consequently, the contributions of the x and y components to the absolute value are less than 10^{-4} times the contribution of the z component. Therefore, we won't introduce an overwhelming systematical error if we only use the z component in our further analysis.

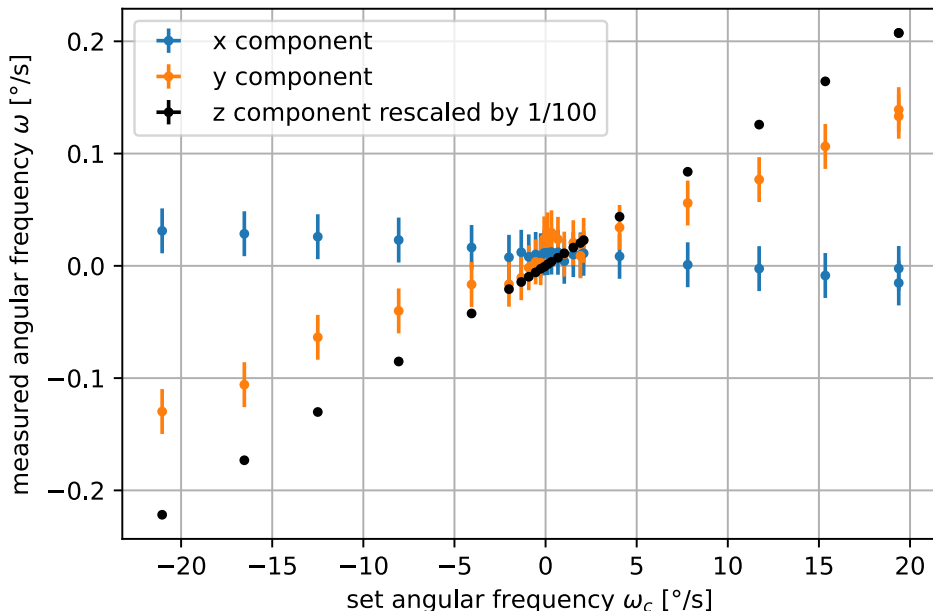


Figure 5: Different components of the measured angular frequency

Having quantified these various statistical and systematical errors, we finally conclude with a comparison of the angular frequencies set at the velocity controller with the ones that the smartphone sensor measured. The values are plotted against each other in fig. 6

The measured values are indeed approximately proportional to the preset angular velocities, but they are not identical: The smartphone sensor gives systematically higher (absolute) values than expected, which is clearly visible in fig. 7 where only the deviations are plotted. Interestingly, the data follow a linear, proportional relation only for values $\geq -10^\circ/\text{s}$. Below that, there is a constant offset. Reaching up to $1.3^\circ/\text{s}$, the errors are much larger than all of the uncertainties discussed above. It seems like the sensor is simply poorly calibrated. Based on our data, we can recalibrate it. First, we perform a linear fit ($\Delta\omega = a_1\omega$) for all values $> -10^\circ/\text{s}$ and one with an additional offset for values $< -10^\circ/\text{s}$. Comparing the resulting parameters, we see that the gradients are indeed approximately the same. As a calibration, we use therefore

$$\omega_{\text{real}} = \omega_z - \Delta\omega = (1 - a_1) \cdot \omega_z = 0.937(3)^\circ/\text{s} \cdot \omega_z.$$

With this calibration, the data up to $-10^\circ/\text{s}$ are well described within their uncertainties ($\chi^2/\text{dof} \approx 1.4$). Only for values $< -10^\circ/\text{s}$, this simple model fails due to the significant offset $b \approx 0.35^\circ/\text{s}$.

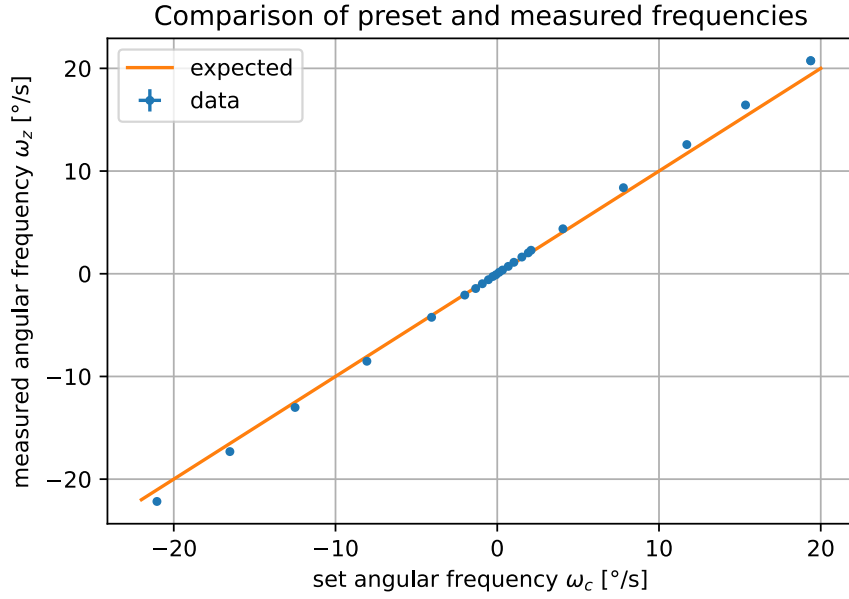


Figure 6: Measured angular velocities (z component) versus the preset values

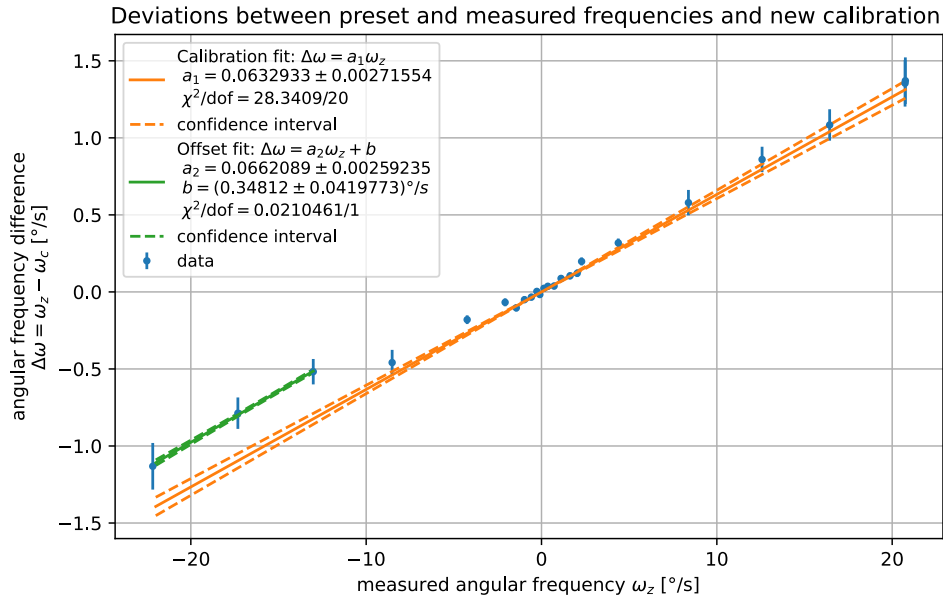


Figure 7: Difference between the measured angular velocities (z component) and the preset values. The calibration fit was performed on the data $> -10^\circ/\text{s}$, the offset fit used only the data $< -10^\circ/\text{s}$.

4.3 Discussion Part 2

We identified and tried to quantify various uncertainties. They include external factors like the axis misalignment that could simply be due to non-horizontal orientation of the whole smartphone. The noise fluctuations that were quantified with the mean uncertainty probably stem from external vibrations and noncontinuous rotation as well as electronic/mechanical noise in the sensor itself. The drift over time in between measurements could be due to something like a temperature change in the electronics. This uncertainty could be analysed in more detail in a more extensive experiment, since it has shown to be the major statistical uncertainty. One could reach a better quantification for it and try to characterise it as either a monotone drift or temporal fluctuations, aiming towards a better understanding of it.

There are also several systematic deviations between the expected and the measured values. On the one hand, the measured frequencies are always larger by roughly 6%. On the other hand,

there is a sudden decrease in $|\omega_z|$ at around $-10^\circ/\text{s}$, resulting in an offset of $b \approx 0.3^\circ/\text{s}$ between different frequency ranges. Given that we measured cw- and ccw-rotations alternately, this change would also influence the values above $+10^\circ/\text{s}$ if it was due to a simple change in external factors. Assuming that the nominal velocities of the stepper motor are correct, that leaves the conclusion that the sensor itself systematically undervalues the velocity above a certain threshold of clockwise rotation in addition to an overall overrating.

Certainly, there could also be other external factors that we couldn't observe or control, like temperature changes, external electric or magnetic fields. Apart from that, the identified uncertainties in order of their estimated magnitude can be summarised as:

- systematic overrating: relative uncertainty ≈ 0.06 , i.e. absolute uncertainty up to $1.2^\circ/\text{s}$
 \leftrightarrow can be compensated via new calibration
- offset between different frequency ranges: $\approx 0.3^\circ/\text{s}$
- drift between measurements ($\Delta t \approx 20 \text{ min}$): $\approx 0.02^\circ/\text{s}$
- noise (mean uncertainty): $\approx 0.0003 - 0.005^\circ/\text{s}$ (depending on number of data points)
- axis misalignment: relative uncertainty $< 10^{-4}$, i.e. absolute uncertainty $< 10^{-3}^\circ/\text{s}$.

The first three factors were identified as characteristic uncertainties of the sensor, only the last two points are directly stemming from uncertainties in the experimental setup and procedure, which means that our experiment was well suited to test the sensor accuracy and sensitivity. Our results indicate that the sensor should be re-calibrated with a factor of $(1-a) = 0.937(3)$ and that it is only accurate in a limited range from $-10^\circ/\text{s}$ (cw) to at least $20^\circ/\text{s}$ (ccw). As a statistical uncertainty, one should always factor in the temporal drift that was around $0.02^\circ/\text{s}$ in our case.

It would be interesting to compare the results from this measurement with another gyroscope, either another MEMS or an entirely different type of gyroscope - e.g. the laser gyroscope, which should perform significantly better than the smartphone sensor.

5 Conclusion

In the first part of this experiment, it was attempted to set up and correctly align a laser gyroscope. The steps undertaken and problems faced were described and a few main learning achievements, as well as possible reasons for why it did not work were discussed.

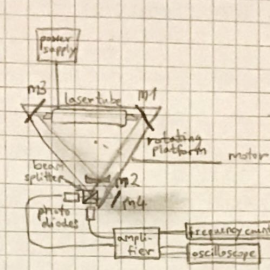
In the second part, we analysed the performance of a smartphone's MEMS gyroscope. Multiple potential sources of uncertainties were discussed, the inherent uncertainties of the sensor were estimated and a new calibration was defined based on the measured data.

References

- [Dem17] Wolfgang Demtröder. *Experimentalphysik 2: Elektrizität und Optik*. 7th ed. Springer Spektrum Berlin, Heidelberg, 2017. DOI: <https://doi.org/10.1007/978-3-662-55790-7>
- [Geb+20] André Gebauer et al. "Reconstruction of the Instantaneous Earth Rotation Vector with Sub-Arcsecond Resolution Using a Large Scale Ring Laser Array". In: *Phys. Rev. Lett.* 125 (2020), p. 033605. DOI: <https://doi.org/10.1103/PhysRevLett.125.033605>
- [Gil+22] Waqas Amin Gill et al. "A Review of MEMS Vibrating Gyroscopes and Their Reliability Issues in Harsh Environments". In: *Sensors* (2022). DOI: <https://doi.org/10.3390/s22197405>
- [Inv] TDK Invensense. *ICM-45686 Datasheet*. URL: https://invensense.tdk.com/wp-content/uploads/documentation/DS-000577_ICM-45686.pdf
- [Las] eLas educational Lasers. *Laserausbildungssystem CA-1310 Laser-Gyroskop Manual*. URL: https://ilias.uni-freiburg.de/goto.php?target=file_3498636_download&client_id=unifreiburg
- [Luh] Photonic Ingenieurbüro Dr Walter Luhs. *LM-0600 HeNe Laser Gyroscope*. URL: https://ilias.uni-freiburg.de/goto.php?target=file_3498629_download&client_id=unifreiburg

6 Appendix A: Signed Lab Notes

Laser Gyroscope



Question: what is the difference between active and passive gyroscopes and which type is better?

- laser already working
- rotating Etalon to find modes ~~~~~ $\Delta \omega$
- seemed to be central mode (no other reflections visible)
- tilt to find next mode (now operating in 1st mode)
- removed 1 diode, looking at overlapping dots on screen
- following manual steps
 - 1) making beams horizontally parallel by turning knobs on BM
 - 2) making beams vertically parallel by tilting BS
 - 3) making them overlap by translating BM
- Seems like system is drifting \ddagger Etalon tilt has to be adjusted every now and then
- only two periodic signals visible on Oscilloscope, but not 180° shifted
 \rightarrow these are not interference signals
- suddenly something wrong with etalon

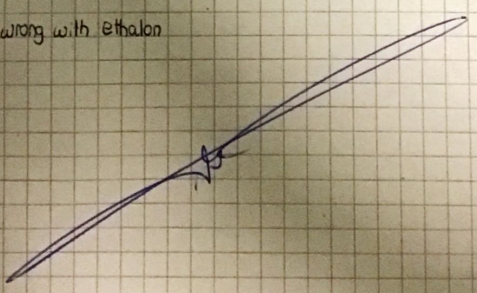


Figure 8: Labnotes Page 1

Measurements with Phyphox (mobile gyroscope)

idea: compare angular velocities stated in manual with angular velocities taken by phone (phyphox app)

placed phone in centre of turntable $t \approx 5s$

Table 1

direction	ω	document name		
ccw	20	"20ccw.csv"	fast $t \approx 5s$	
cw	20	"20cw"		
ccw	16	"16ccw"		
cw	16	"16cw"		
ccw	12	"12ccw"		
cw	12	"12cw"		
ccw	8	"8ccw"		
cw	8	"8cw"		
ccw	4	"4ccw"		
cw	4	"4cw"		
ccw	2	"2ccw"		
cw	2	"2cw"		
ccw	1.8	"1k8ccw"		slow $t \approx 10s$ → higher noise
cw	1.8	"1k8cw"		
ccw	1.4	"1k4ccw"		
cw	1.4	"1k4cw"		
ccw	1.0	"1k0ccw"		
cw	1.0	"1k0cw"		
ccw	0.6	"0k6ccw"		
cw	0.6	"0k6cw"		
ccw	0.3	"0k3ccw"		
cw	0.3	"0k3cw"		
ccw	0.1	"0k1ccw"		
cw	0.1	"0k1cw"		

Figure 9: Labnotes Page 2

to check for drift: repetition
 ccw 20 " 20 ccw 2 "

measurement without motion $t = 20s$ "static"

Back to the laser gyroscope

without etalon: laser working, oscilloscope shows two periodic signals (same phase)
 → make strengths of signals equal by tilting B11
 → screenshot

with etalon: no lasing

"monkey technique": systematically turn both etalon screws by $\frac{1}{4}$ turns, then rotate etalon whole turn and watch oscilloscope for changing signal
 → nothing found

cleaning etalon with acetone
 no obvious damages visible
 green laser passes etalon without any effect (as expected)

"monkey 2": first change lower screw by a bit, then simultaneously turn rotation wheel and upper screw (through full range). Repeat

Mounting green laser again to check alignment
 ↳ noticed that additional weight of laser also stops lasing of red laser
 How much sense does it make then to use green laser?

next idea: start laser alignment (with green laser) from the beginning, following steps in the manual

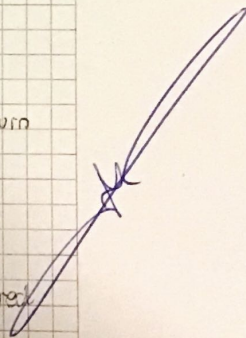


Figure 10: Labnotes Page 3

Optimization of laserpower: turning one screw at a time and going through all mirrors

Trying to insert the etalon again

↳ very sensitive! possible to get lasing before pushing the etalon fully into the holder

trick: align green and red laser, then try to get back reflection of green laser to overlap with incoming green forward reflection

trick2: unscrew whole etalon holder and move slightly to find good etalon position

~~05.09.2024~~

Figure 11: Labnotes Page 4

7 Appendix B: Additional Pictures and Data

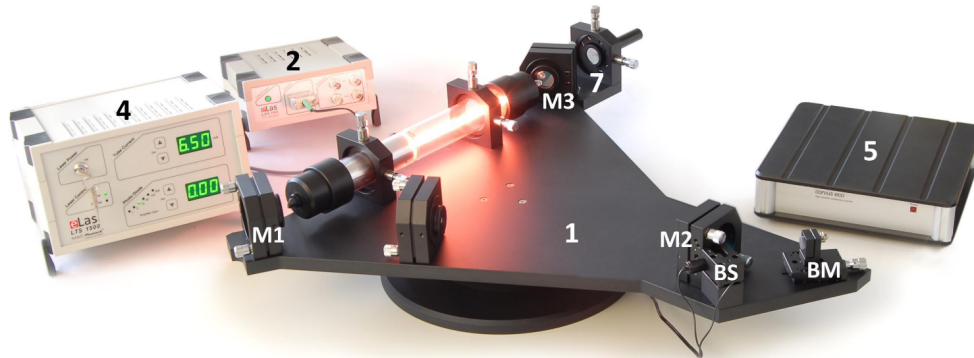


Figure 12: Labelling of the components of the laser gyroscope. This picture is taken from chapter 2 of the manual [Las](#).

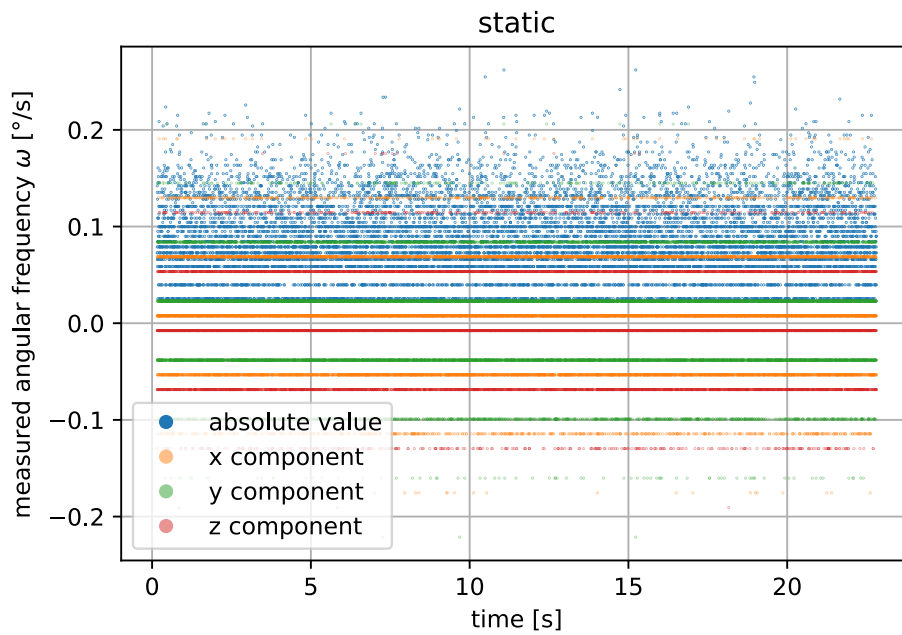


Figure 13: Angular momentum measured with the smartphone gyroscope at zero rotation

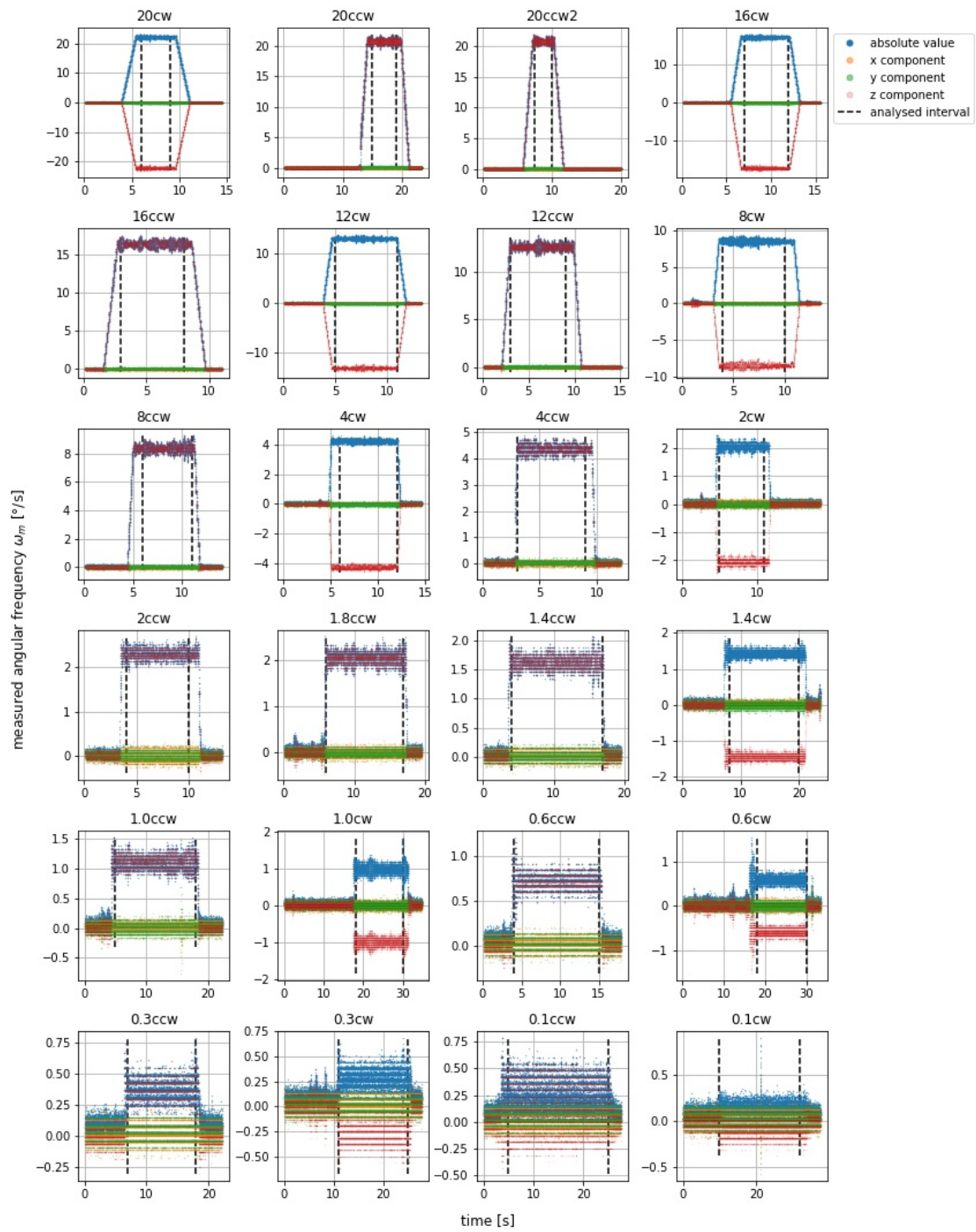


Figure 14: Data from the rotation measurements with the smartphone gyroscope. Plot titles indicate approximate rotation speed (in $^{\circ}/s$) and direction ((c)cw: (counter-)clockwise).